Escamilla, P.; Guerra, WD.; Leyva Perez, A.; Armentano, D.; Ferrando-Soria, J.; Pardo, E. (2023). Metal-organic frameworks as chemical nanoreactors for the preparation of catalytically active metal compounds. Chemical Communications. 59. https://doi.org/10.1039/d2cc05686k

ARTICLE

Metal-organic frameworks as chemical nanoreactors for the preparation of catalytically active metal compounds

Received 00th January 20xx,
Accepted 00th January 20xx

DOI: 10.1039/x0xx00000x

Paula Escamilla,[a] Walter Guerra,[a] Antonio Leyva-Pérez,[b] Donatella Armentano,[c] Jesús Ferrando-Soria,*[a] Emilio Pardo*[a]

Since the emergence of metal-organic frameworks (MOFs), a myriad of thrilling properties and applications, in a wide range of fields, have been reported for these materials, which mainly arise from their porous nature and rich host-guest chemistry. However, other important features of MOFs that offer great potential rewards, have been only barely explored. For instance, despite the fact that MOFs are suitable candidates to be used as chemical nanoreactors for the preparation, stabilization and characterization of unique functional species, that would be hardly accessible outside the functional constrained space offered by MOF channels, only very few examples have been reported so far. In particular, we outline in this feature recent advances on the use of highly robust and crystalline oxamato- and oxamidato-based MOFs as reactors for the *in-situ* preparation of well-defined catalytically-active single atom catalysts (SACS), subnanometer metal nanoclusters (SNMCs) and supramolecular coordination complexes (SCCs). The robustness of selected MOFs permits the post-synthetic (PS) in-situ preparation of the desired catallytically-active metal species, which can be characterised by single-crystal x-ray diffraction (SC-XRD) taking advantage of its high crystallinity. The strategy highlighted here permits the always challenging large-scale preparation of stable and well-defined SACs, SNMCs and SCCs, exhibiting outstanding catalytic activities.

1. Introduction

Metal-organic frameworks (MOFs)[1–5] are crystalline porous materials self-assembled by the combination of metal cations/metal clusters with a seemingly limitless variety of organic spacers. As a direct consequence, MOFs reported so far, offer a wide variety of intriguing net topologies and fascinating porous high-dimensional structures with thrilling host-guest chemistry.[6,7] As a result, MOFs have found application –given their unique chemical and physical properties[5]– in such diverse fields as gas storage and separation,[8] transport,[9] drug delivery,[10] molecular recognition,[11] water remediation[12] or catalysis,[13] and, more recently, as templates for the encapsulation of metal nanoparticles (MNPs)[14] and a wide variety of other functional moieties.[15]

Regarding encapsulation skills of MOFs, there are several reasons that explain such efficiency. Apart, from the high surface areas and pore volumes of MOFs, they exhibit suitable functionalities decorating their channels –that can be fine-tuned during their synthesis or in a post-synthetic (PS) treatment[16]– capable to establish covalent bonding or van der Walls multiple interactions with target guest molecules. Thus, a plethora of metal nanoparticles,[14,17–21] metal complexes[22–29] and organic (macro)molecules[30–32] have been efficiently encapsulated. For example, the blooming growth of this field is nicely illustrated in Fig. 1, where we have represented the number of publications focused on the encapsulation of single atom catalysts (SACS), subnanometer metal nanoclusters (SNMCs) and supramolecular coordination complexes (SCCs) within MOFs channels in the 2015-2022 period.

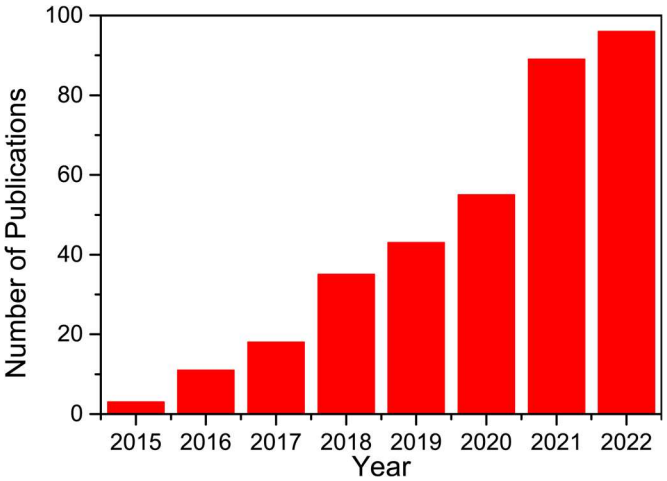

Fig. 1. Number of publications related to the MOF encapsulation of single atom catalysts (SACS), subnanometer metal nanoclusters (SNMCs) and supramolecular coordination complexes (SCCs) in the 2015-2022 period.

In this context, the group of Prof. Makoto Fujita has recently gone one step further on the guest encapsulation in MOFs, developing the so-called "crystalline sponge method".[11,33,34] Essentially, this approach consists on the use of suitable

[a] *Instituto de Ciencia Molecular (ICMol), Universidad de Valencia, 46980 Paterna, Valencia, Spain. E-mail: jesus.ferrando@uv.es; emilio.pardo@uv.es.*
[b] *Instituto de Tecnología Química (UPV-CSIC). Universidad Politécnica de Valencia-Consejo Superior de Investigaciones Científicas, 46022 Valencia (Spain)*
[c] *Dipartimento di Chimica e Tecnologie Chimiche, Università della Calabria, 87036 Rende, Cosenza, Italy.*

selected MOFs as ”vessels” to encapsulate molecules, which fit perfectly within the MOFs cavities. Thus, such use of MOFs as molecular flasks allows the perfect immobilization of guest molecules, reducing disorder and enabling the structural resolution of molecules with unknown structure. Other more recent works,[35–38] following the path traced by this strategy, have deepened on the design of MOFs channels. Focusing on their functionalization, in order to optimize the host-guest interactions and, ultimately, the immobilization and ordering of the guest molecules.[39]

In contrast to the great attention and remarkable advances on the encapsulation of functional species within MOFs channels, other promising features of these materials have been barely explored. In particular, MOFs also offer great possibilities for the *in-situ* preparation of unique functional species by taking advantage of the unique confined space and functional environment that their channels may offer.[40,41] Thus, acting as effective chemical nanoreactors. Alternatively, MOFs can be also used as sacrificial agents to obtain MOF-derived carbonaceous materials doped with single atom catalysts and sub-nanometer metal nanoclusters. Despite the fact that we will focus on the use of MOFs as chemical reactors, we refer the eager reader to some recent published reviews based on the second strategy.[42–45]

Traditionally, a chemical nanoreactor has been defined as a nanosized container where a chemical reaction takes place.[46] This classical definition has been somehow expanded when applied to MOFs. Thus, a MOF nanoreactor should not be regarded as a simple vessel where reactants combine to form products. Indeed, a MOF nanoreactor offers a functional confined space that may play a fundamental role on the chemical processes that occur inside the channels, by controlling the number and orientation of molecules and their non-covalent interactions, similarly to that observed in nature within natural nanoreactors.[46] These characteristics allow a certain synthetic control to form unique metal species within this functional constrained space, thus endowing MOF-reactors with a dual role: (*i*) Firstly, MOFs can act as a chemical reactor to form unique catalytic metal species –difficult to be obtained in solution- that are efficiently stabilized and retained within their pores. (*ii*) Secondly, such formed novel metal species are used as catalysts in challenging organic reactions, taking advantage of the functional limited spaces where catalysts are hosted, rendering interesting selectivities and higher reusabilities.

2. General synthetic strategy

Prior to describe how a MOF can be used as a chemical nanoreactor to prepare catalytically active metal species inside their pores, we must answer/define, unambiguously, two questions: what type of species are suitable to be prepared and why using a MOF as chemical reactors is the best strategy to achieve them. The answer to both of them is the same: They must be species that cannot be easily prepared and stabilised outside MOFs channels. In this context three types of species appear as optimal species. They are ligand-free single atom

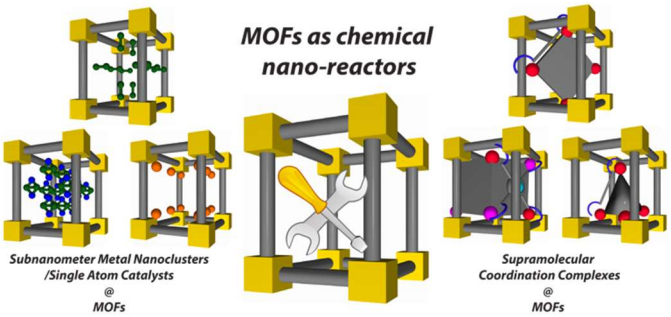

catalysts (SACS),[47,48] subnanometer metal nanoclusters (SNMCs)[49,50] and supramolecular coordination complexes (SCCs)[51–54] or even other supramolecular species (Fig. 2).

Fig. 2. Schematic representation of the possible metal compounds synthesised using MOFs as metal nanoreactors that are highlighted in this feature. This includes homo- and heterometallic subnanometer metal nanoclusters (left) and supramolecular coordination complexes (right).

In particular, small aggregations of less than 10 metal atoms, falling within the sub-nanometric regime that include SACs and SNMCs,[55] are called to promote a paradigmatic shift in technology, as happened before with metal nanoparticles (MNPs).[56–58] These ultra-small entities offer enormous potential applications that may be relevant in different technological areas of interest,[59–62] particularly in catalysis. Among the reasons for this potential in catalysis, the most obvious is related to their small size, which lead to all atoms being outer exposed and interacting between them,[55] and consequently, to a thrilling catalytic activity.[50,63–73] However, despite their exciting possibilities, their synthesis, even at the milligram scale, is extremely difficult. It is complicated to synthesise and, especially, stabilise such metal species without protective ligands, whose presence would decrease dramatically their catalytic activity. Here is where MOFs, acting as chemical nanoreactors, could play a dual fundamental role: in the challenging controlled preparation of ligand-free SACs and SNMCs, and, especially, in the stabilization of these species without protective stabilizing ligands –considering that the multiple weak interactions stablished between the guest metal species and the host functional framework help to maintain the metal species’ integrity, without altering their catalytic properties. On the other side, a smart use of supramolecular chemistry[74] has also led to a good number of fascinating examples of supramolecular coordination compounds (SCCs) –*i.e*. metal-organic polygons and polyhedra– with thrilling functionalities, sometimes reminiscent to those present in living beings.[75] However, their technological interest –*i.e*. catalysis– has been somehow hampered by a very frequent weak structural robustness of the formed species under working conditions, as they have been usually limited to homogenous chemistry in solution. Again, here, MOFs as chemical nanoreactors arise as a suitable alternative, not only to prepare unique SCCs –different to those that would be formed in solution–but also to stabilize SCCs improving their catalytic performances.

Once defined that SACs, SNMCs and SCCs are the most suitable candidates to be prepared (and stabilised) using MOFs as chemical nanoreactors, we can describe the general synthetic strategy. This is based on the consecutive application of post-synthetic methodologies (PSMs), for the step-by-step construction of these species (Fig. 3) within the functional confined space offered by selected MOFs (see point 3). Overall, the synthetic strategy can be broadly divided in two main points: (*i*) The insertion of metal cations within the channels of the MOF reactor and (*ii*)/(*iii*) the application of different consecutive PS steps for the preparation of SACs/SNMCs on the one side or SCCs on the other.

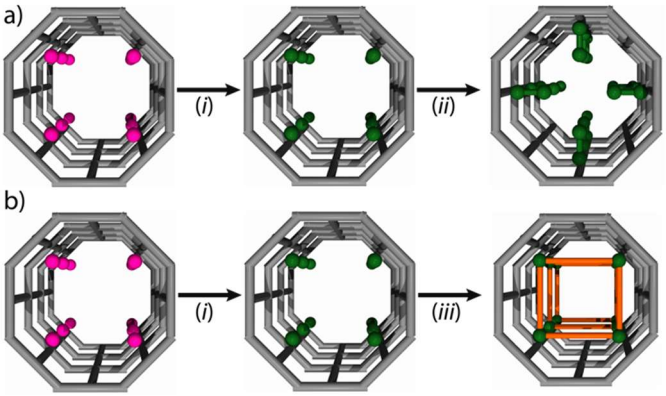

Fig. 3. Post-synthetic strategy for the MOF driven preparation of SNMCs/SACs (a) and SCCs (b): (*i*) post-synthetic insertion of metal cations within the MOFs channels, (*ii*) post-synthetic chemical reduction of inserted metal cations to render SACs/SNMCs and (*iii*) post-synthetic insertion of suitable ligands to build SCCs.

Controlled insertion of metal cations within MOFs channels

A successful development of the general strategy for the preparation of well-defined ligand free SACs/SNMCs and SCCs relies, first, on the controlled insertion of a limited number of metal cations within the channels of the MOF reactor (Fig. 3a and 3b, part (*i*)). Indeed, this point is of particular relevance for preventing the formation of large MNPs –as usually happens with other methodologies, such as "metal impregnation methods". In this context, MOFs seem to offer better performances than other porous materials to control metal stoichiometry, as the number of metal cations inserted can be controlled either by the charge of the framework and/or the functionalities decorating their pores (see point 3). These MOF features also appear relevant for another characteristic of fundamental importance during the insertion process, the metal location. Indeed, certain reported examples[76,77] indicate that inserted metal cations occupy specific unique positions –depending on the nature of the metal cation– within the channels, as they interact with the rationally introduced functionalities decorating them. This is of paramount importance because allow a homogeneous distribution of metals along the channels, which, in turn, favours the formation of discrete metal compounds and, in addition, facilitates the use of single-crystal X-ray diffraction (SCXRD) to unveil the positions/distances of these metals, and thus, the application of PSMs in the second step.

Application of PSM to prepare SACs/SNMCs or SCCs

Once a limited number of metal cations are inserted within MOFs' channels, occupying specific positions –tentatively unveiled by SCXRD–, two main approaches can be followed either to obtain SACs/SNMCs (Fig. 3a, part (*ii*)) or SCCs (Fig. 3b, part (*iii*)), having in common the use of PSMs to achieve the final species:

(*ii*) The preparation of SACs/SNMCs is achieved under the controlled insertion of a reducing agent within the channels where metals are hosted. The accumulative weak interactions established between the metal cations and the channels functionalities are not only useful to control the number of metals that are inserted, but also, to restrain the movement of metals during the reduction process. Both factors are crucial to ensure the formation of very small naked SNMCs (and even SACs), preventing the formation of larger MNPs, that are homogeneously distributed along the channels, occupying specific positions and allowing that no protective ligands are necessary since metal clusters are stabilised by the MOF itself.

(*iii*) The design of SCCs relies on the PS insertion of suitable ligands, which can lead to the formation of unprecedented SCCs and other supramolecular constructs by taking advantage of the unique confined functional space offered by MOFs. Herein, the ligand suitability is determined with the key help of SCXRD, allowing to unveil metal atom positions and distances, which are parameters of fundamental importance to select most appropriate ligands for insertion. Overall, the preparation of SCCs within MOF reactors permits two remarkable facts: the assembly of unique supramolecular species –that can only be synthesised within this constrained space– and an enhancement of their structural stability –assisted and supported by weak noncovalent interactions established with the framework– with the concomitant improved catalytic behaviour.

3. Design of suitable MOFs to be used as chemical reactors

General characteristics

Aiming at using MOFs as chemical reactors (MOF-reactors) to (*i*) synthesise unique catalytically active metal species within their pores, and (*ii*) carry out organic reactions where preformed metal species act as catalyst, it is essential to define the characteristics that a given MOF must have for this purpose. Suitable MOF-reactors should provide the appropriate environment to grow, in a gram-scale, SACS, SNMCs and SCCs. In order to do so, they can take advantage either of the functionalities of the channels or the charge of the framework to anchor metal cations to the walls, as well as of the nanostructured confined space to limit the size of the formed species and also offer size-selectivities in catalysis (see point 2).

Thus, a fine tuning of both functionalities decorating the pores and their size (and shape) should be somehow ensured. Moreover, once metal cations are inserted within MOFs channels, further PS steps will be employed to synthesise SACs/SNMCs/SCCs, and thus, a high degree of robustness is required to ensure that MOFs maintain their integrity under

these sometimes harsh conditions (see point 2). This point is particularly important. Indeed, MOFs must present high chemical stability not only to resist PSMs but also to resist reaction conditions if used in catalysis. This is achieved by a careful choice of ligands (which must be stable a plethora of solvents and in a wide interval of temperatures) and also using metals with high oxidation states. In particular, a wide diversity of Cr^{III},[78] Zr^{IV},[79–81] Ti^{IV},[82,83] etc. Finally, certain MOFs offer the possibility to use SCXRD as a powerful tool to shed light on the crystal structure of both starting preformed MOFs and the final host-guest aggregate. Therefore, the use of highly crystalline MOFs provides a better chance to use SCXRD on the formed catalytically active species.

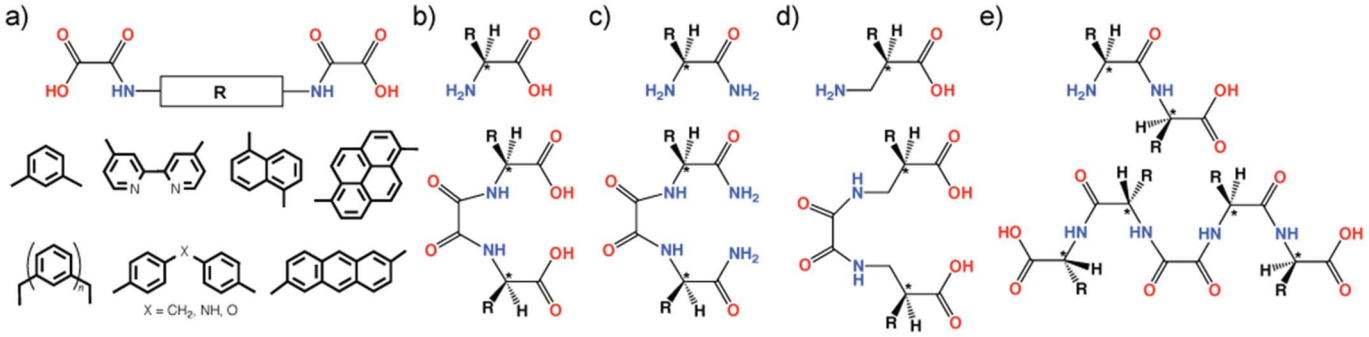

Fig 4. Selected general examples of oxamate- and oxamidate-based ligands derived from robust and flexible aromatic diamines (a), α-amino acids (b), their amide derivatives (c), β-amino acids (d) and oligopeptides (e) that have been used to prepare oxamato and oxamidato based MOFs. In particular, in this review we present MOFs derived from aromatic diamines and amino acids.

In particular, we have devoted our efforts, in recent years, to the design of novel families of MOFs using oxamate- and oxamidate ligands aiming at their use as chemical nanoreactors. Indeed, these ligands have demonstrated high versatility to build both anionic and neutral functional MOFs.[39,84–89] These families of ligands can be either derived from robust aromatic amines or from biomolecules such as chiral amino acids (Fig. 4), which afford very stable "metalloligand" complexes capable to build, in a rational manner and in large scale, these highly robust water-stable functional MOFs.[86] Moreover, these ligands offer the possibility to provide a controlled functionalization of the channels, which, as seen in point 2, is crucial to retain metal cations in specific positions and also to somehow control the formation of SACs/SNMCs/SCCs. Last but not least, oxamato- and oxamidato-based MOFs have already proven highly crystalline. This last point, does not only mean that we are capable to unveil the crystal structure of pristine MOFs, but also that the single crystals of these MOFs, capable of maintaining their integrity after the consecutive application of PSMs, and the crystal structure of host-guest materials containing SACs/SNMCs/SCCs, can be sometimes ascertained.

Multivariate MOFs

There is a particular type of MOFs –so-called multivariate MOFs[90–92] (MTV-MOFs)– that may become particularly relevant for the preparation of certain kinds of species, in particular heterometallic SNMCs and SCCs, using these MTV-MOFs as chemical nanoreactors. The chemical approach that we have followed for the preparation of MTV-MOFs is based on the use of different types of metalloligands, prepared with oxamidato-based organic linkers derived from amino acids. This has allowed us the fabrication of isoreticular MOFs with different and controlled functionalities within their channels (Fig. 5). This type of sequence-dependent materials,[93] are thus capable, in principle, of new functions without apparent loss of synthetic control. For example, we can take advantage of the different functionalities decorating the channels, to incorporate two or more metals of different nature expecting that they interact, differently, with the distinct functional groups. In doing so, we can not only control the ratios of inserted metals, but also, we expect that they occupy specific different positions. Then, heterometallic SNMCs and SCCs can be constructed after the application of sequential PSMs.

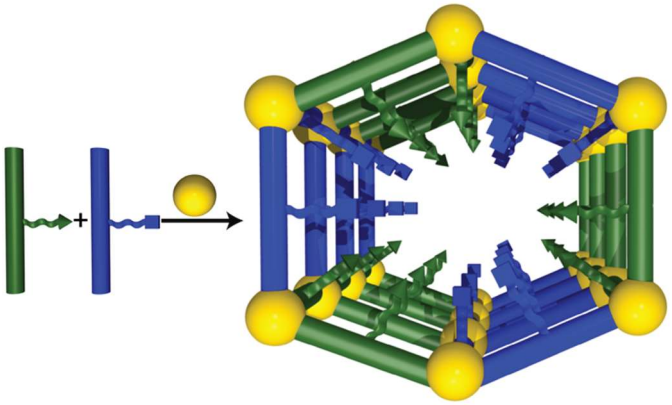

Fig. 5. Schematic representation showing the design strategy proposed to prepare MTV-MOFs. Each different metalloligand has been depicted as using different color sticks (green and blue) and the metal ions as yellow spheres. The different proposed ligands can be found in Fig. 4b-e.

In particular, we have prepared a battery of isoreticular oxamidate MTV-MOFs by combining different percentages of metalloligands with oxamidato-based amino acids, which, in principle, should allow the rational insertion of metals of different nature. For example, thioether groups from *L*-methionine or *S*-methyl-*L*-cysteine are expected to show higher affinity for noble metals, whereas oxygen or nitrogen-containing functional groups will preferentially interact with transition metal cations (Fig. 6).

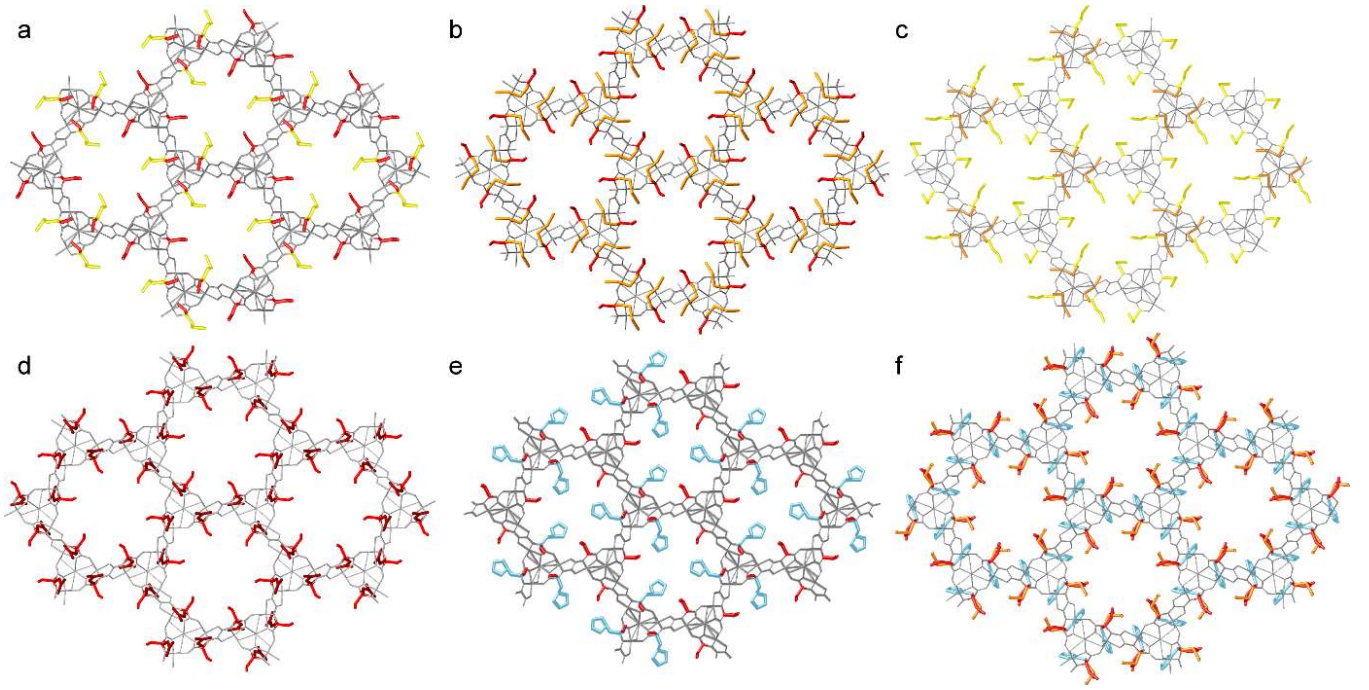

Fig. 6. Selected examples of recently synthesized oxamidate-based MTV-MOFs containing the following amino acids: *S*-Methyl-*L*-cysteine (yellow) / *L*-serine (red) (a), *L*-methionine (orange) / *L*-serine (red) (b), *S*-Methyl-*L*-cysteine (yellow) / *L*-methionine (orange) (c), aspartic acid (dark red) / *L*-serine (red) (d), *L*-histidine (blue) / *L*-serine (red) (e), *L*-histidine (blue) / *L*-serine (red) / *L*-methionine (orange) (f).

4. Preparation/stabilization of SACs and SNMCs

The proposed synthetic strategy (points 2 and 3), consisting on the use of highly crystalline and robust oxamato- and oxamidato-based MOFs, as chemical reactors, has proven successful during recent years to prepare, stabilise and characterise different examples of MOF-driven SACs and homometallic SNMCs**.** Indeed, this success is assessed by a good number of striking published results[38,84,87,89,94–100] that are highlighted below.

MOF-driven formation of SNMCs

Our first publication in the field was based on the use, as chemical nanoreactor, of a highly robust anionic oxamato-based MOF of formula $Ni^{II}_2\{Ni^{II}_4[Cu^{II}_2(Me_3mpba)_2]_3\}$ [where Me_3mpba^{4-} = *N,N'*–2,4,6–trimethyl–1,3–phenylenebis(oxamate)] (Figs. 3a and 6a) to synthesize ligand-free subnanometer tetranuclear palladium clusters after two consecutive PS steps.[84] Remarkably, the structure of such ultrasmall Pd SNMCs could be unveiled by SCXRD, offering unique snapshots about the nature of these tiny species and also about the stabilizing interactions established with the framework (Fig. 7). This dual PS strategy consisted first on the replacement of Ni^{II} cations by $[Pd^{II}(NH_3)_4]^{2+}$ ones, yielding an intermediate MOF with formula $[Pd^{II}(NH_3)_4][Pd^{II}_2(\mu\text{–}O)(NH_3)_6)(NH_4)_2]_{0.5}\{Ni^{II}_4[Cu^{II}_2(Me_3mpba)_2]_3\}$, which hosts Pd^{II} cations in specific positions within the channels by interacting with carboxylate oxygen atoms from the network (Fig. 7b). Then, in a second step, Pd^{2+} cations are reduced after controlled insertion of $NaBH_4$, giving rise to the final hybrid material of formula $[Pd_4]_{0.5}@Na_3\{Ni^{II}_4[Cu^{II}_2(Me_3mpba)_2]_3\}$ (Fig. 7c). Remarkably, the resolution of the crystal structure of the subnanometer linear Pd_4 clusters –within MOFs channels– constituted a very significant step forward in the characterization of these small species. Its structure confirmed, for the first time, that Pd_4 clusters were stable without the need of using blocking protective ligands, being the MOF itself responsible for maintaining their integrity. As a consequence, all palladium atoms are outer-exposed, which offers great potential for catalysis. Moreover, these linear $[Pd_4]^{2+}$ SNMCs are homogeneously distributed along the channels occupying positions where host-guest interactions are maximized. Interestingly, these non-covalent forces show a trade-off behaviour, being strong enough to stabilize and spatially organise the generated $[Pd_4]^{2+}$ species –endowing valence on metals otherwise not stable– and at the same time, weak enough to not impact on their catalytic active surface.

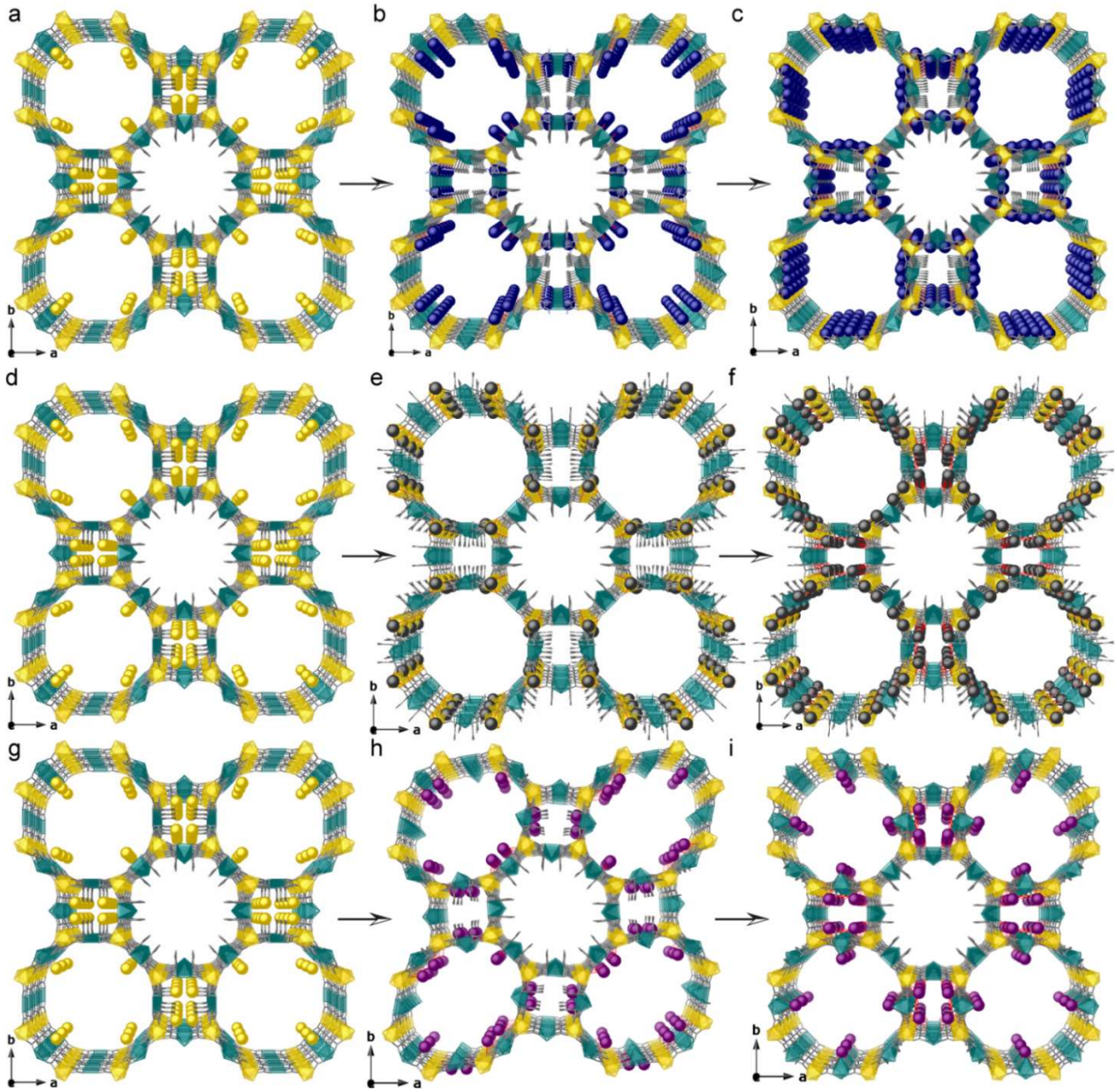

Fig. 7. Two–step PS approach for the synthesis of $[Pd_4]^{2+}$, Ag^0_2 SNMCs and Pt^I SACs consisting of (*i*) the susbstitution of Ni^{II} cations (yellow spheres) hosted in the channels of Cu_6Ni_6 MOF (a and d) by Pd^{II} (blue spheres), Ag^I ones (grey spheres) or Pt^{II} (purple spheres) to give the intermediate MOFs $Cu_6Ni_4Pd_2$ (b), $Cu_6Ni_4Ag_4$ (e) and $Cu_6Ni_4Pt_2$ (h), followed by (*ii*) the concomitant reduction of Pd^{II}, Ag^I and Pt^{II} cations to give $[Pd_4]^{2+}$ (c) and Ag^0_2 (f) SNMCs or Pt^I SACs (i). Red dotted lines indicate weak non-covalent interactions of the metal units with the carboxylate oxygen atoms from the network.

Aiming at unveiling the catalytic activity of $[Pd_4]^{2+}$ SNMCs, they were tested towards the Buchner ring expansion reaction and other carbene insertion reactions. Indeed, these ligand free SNMCs exhibited outstanding catalytic activity/recyclability for these reactions (yields higher than 90% in all cases, turnover numbers close to 100000 and, at least, 20 reuses), surpassing by more than one order of magnitude the state of the art rhodium catalysts.[101] Overall, this pioneering work demonstrated that the gram-scale preparation of ligand-free SNMCs was feasible using MOFs as nanoreactors, without loss of catalytic activity and, in turn, enhancing the chemical stabilities of these tiny metal species.

The same anionic CuNi MOF was later used –following the same synthetic strategy– for the *in-situ* preparation of ligand-free Ag^0_2 SNMCs[102] (Figs. 6d-f), the whole formation process being also followed by SCXRD. Again, the anionic charge of the framework was crucial to limit the number of inserted silver(I) cations.[102] Remarkably, a close inspection of the crystal structures of the MOF with Pd^{II} (Fig. 7b) and Ag^I (Fig. 7e) allows to confirm that metal cations occupy different specific positions within the channels by interacting with different carboxylate oxygen atoms of the MOF. We strongly believe that these different positions, that metals of different nature occupy, lie at the origin of the different nuclearity that we observe for different SNMCs, such as for example Ag_2 and Pd_4. This is also

intimately connected to the limited and restrained movement that these metals have during the cluster formation process –as they are anchored to the walls of the MOF. In any case, despite possessing a different nuclearity both, Ag_2 and Pd_4, are ligand free subnanometer nanoclusters, with all atoms exposed to reactants, and an outstanding catalytic activity can be expected for Ag_2. In this context, Ag_2 SNMCs we are also tested for the Buchner ring expansion reaction showing catalytic results approaching those observed for Pd_4 SNMCs, which, considering the lower prices and higher abundance of silver, can indeed provide important advantages.

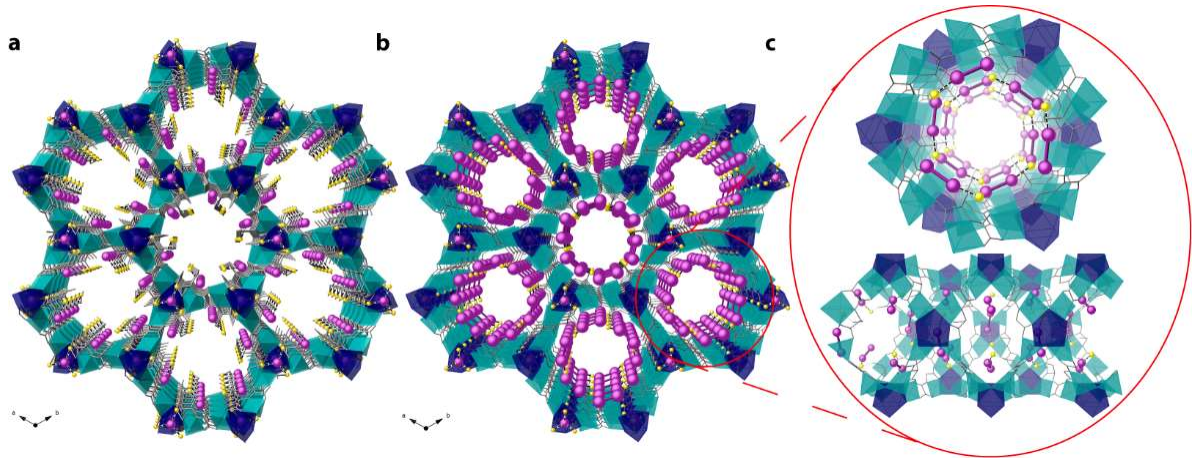

Fig. 8. Crystal structures of the Pt^{II}@MOF (a) and Pt^0_2@MOF (b), determined by SCXRD. c) Perspective views, in detail, of a channel of Pt^0_2@MOF. Copper and calcium atoms from the network are represented by cyan and blue polyhedra, respectively, whereas organic ligands are depicted as grey sticks. Yellow and purple spheres represent S and Pt atoms, respectively. Dashed lines represent the Pt···S interactions.

The MOF-directed preparation of Pd and Ag SNMCs described above is based on a controlled insertion of metals whose number is limited by the anionic charge of the MOF. This crucial point can be also controlled in neutral MOFs if their channels are decorated with suitable functional groups. This is perfectly illustrated when selecting an oxamidato-based MOF, derived from natural amino acid *L*-methione, of formula $\{Ca^{II}Cu^{II}_6[(S,S)\text{-methox}]_3(OH)_2(H_2O)]$ (where methox = bis[(*S*)-methionine]oxalyl diamide), whose channels are densely decorated with thioether groups. On the basis that sulphur containing groups have affinity for certain soft metals, thioether groups decorating the channels can be used to insert a limited number of noble metals within the channels, offering also a very homogeneous distribution for them, as they remain anchored to specific positions defined by these functional groups. Therefore, following a very similar two-step PS approach, we reported the gram-scale preparation of Pt^0_2 SNMCs, process that could be followed with SCXRD.[103] First, *L*-methionine MOF was immersed within a Pt^{II} solution. As expected, a high loading of Pt^{II} –densely-packaged and homogenously distributed along the channels– could be observed (Fig. 8a). Such homogeneous distribution of Pt^{II} cations play a key role –in combination with the small confined empty space of the chemical reactor and the restrictions of movement of anchored Pt^{II} cations– in the controlled formation of ligand-free ultrasmall SNMCs instead of larger MNPs. Therefore, Pt^{II} cations are reduced in the presence of a chemical reducing agent ($NaBH_4$) giving rise to ligand-free well-defined Pt^0_2 SNMCs that are, again, anchored to the sulphur-containing groups decorating the pores, thus being homogeneously distributed along the channels, as unveiled by SCXRD (Fig. 8b,c).

The example mentioned before is also illustrative of how the flexibility of the MOF can play a fundamental role in the cluster formation, as thioether groups from *L*-methionine ligands are long and flexible enough to approach two Pt^{II} cations to form the dinuclear cluster, but, at the same time, are isolated enough to prevent the formation of larger nanoclusters or MNPs.

As we expected, the resulting naked Pt^0_2 nanoclusters proven themselves highly active in three potentially important industrial reactions, such as CH_4 from CO_2, cyanide production and selective ethylene hydrogenation.

MOF-driven formation of SACs

The same strategy described for the preparation of SNMCs may lead also to the preparation of MOF-driven SACs embedded within the channels. Herein we report two examples obtained using both the oxamato-based anionic CuNi MOF and also an oxamidato-based neutral MOF functionalised with thioether groups.

The first example consists on the gram-scale preparation of well-defined platinum(I) SACs stabilised by water clusters. The first step of the PS process consisted on the insertion, within the channels of $Ni^{II}_2\{Ni^{II}_4[Cu^{II}_2(Me_3mpba)_2]_3\}$ MOF, of a controlled number of Pt^{II} cations (Fig. 7h) that replace Ni^{II} cations and occupy, as happened for Pd^{II} and Ag^{I}, unique specific positions (Fig. 7b,e). Then, after reduction with $NaBH_4$, Pt_1^{1+} SACs are formed and stabilized within the confined functional channels, as unveiled by SCXRD (Fig. 7i). This is the second example reported in this revision where unusual oxidation states are observed for SNMCs/SACs formed within this anionic MOF, which suggest that this porous material is not only suitable to form/stabilize metal nanosized species with regular oxidation states, but also possessing uncommon ones. In this sense, it has been unveiled that the water cluster surrounding Pt_1^{1+} SACs

helps to stabilize the Pt SACs and also regulates the charge of the metal.

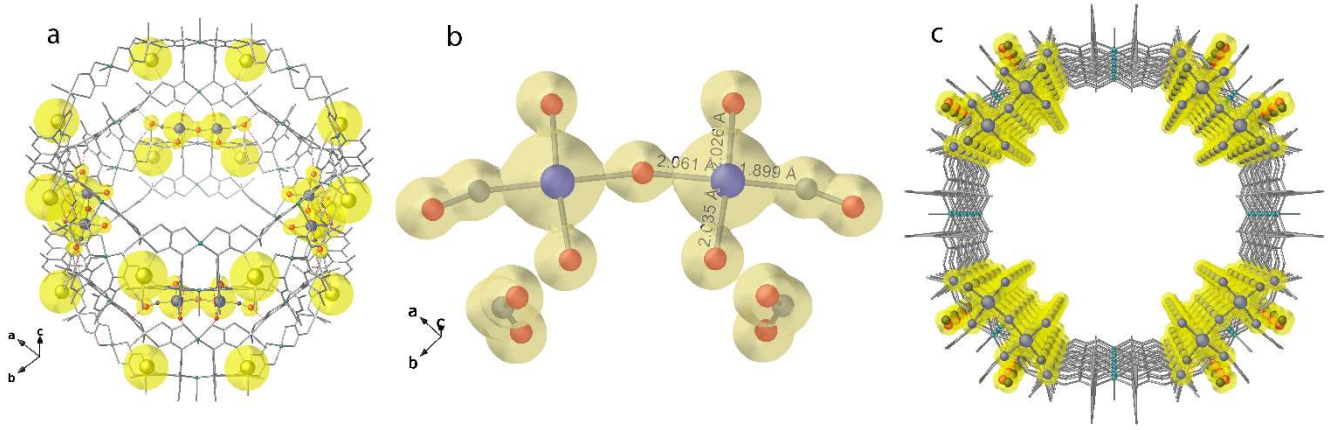

Fig. 9. Perspective views showing details of the crystal structure of Pt_1^{1+}@MOF crystal structure with CO molecules embedded: a) single pore side view of hydrogen bonds interactions stabilizing $[Pt^{1+}_2(\mu\text{-}O)(CO)_2(H_2O)_4]$ intermediates within hydrophilic pores; b) detailed crystal structure of $[Pt^{1+}_2(\mu\text{-}O)(CO)_2(H_2O)_4]$ moieties clarifying CO and H_2O binding sites; c) view down direction of pore's propagation showing (all in blue color) the *in-situ* generated molecules interacting with MOF's walls. Na^+ and Pt^+ in gold and blue ones, respectively. The heterobimetallic CuNi 3D anionic network is depicted as grey sticks. Carbon and oxygen atoms of the *in-situ* generated molecules, are depicted as grey and red spheres, respectively. Surface has been depicted to highlight Pt-CO water adducts and CO_2 hosted in pores. This figure is reproduced with permission from ref. 104, copyright Wiley and sons 2021.

The catalytic activity of Pt_1^{1+} SACs was also evaluated. For that, this peculiar oxidation state of platinum was taken into consideration, and a potentially important industrial reaction, such as the water–gas shift reaction (WGSR: $CO + H_2O \rightarrow CO_2 + H_2$), was selected. As we expected, Pt_1^{1+} SACs showed great catalytic performance for the WGSR at very low temperature (50 °C). Apart from this catalytic efficiency, in a concomitant communication, we were capable to establish a plausible catalytic mechanism.[104] This consisted on a double water attack to CO –from both a water molecule coordinated to the metal coordinated and also a H–bonded one– yielding CO_2 with both oxygen atoms coming from water. In fact, we could follow the reaction by using *in-operando* SCXRD. This allowed to visualize the formation of a hemiacetal intermediate, where two H_2O molecules are added to CO on the Pt_1 catalyst (Fig. 9). This confirmed our previous predictions, and even more relevantly, provided a paradigmatic shift in the assumed mechanism of the WGSR.

MOF-driven SACs can be also synthesized using neutral MOFs. In particular, we used an oxamidato-based MOF, prepared from the amino acid *S*-methyl-*L*-cysteine (Fig. 10a), to prepare Pd^0_1 SACs.[105] The 3D MOF, with formula $\{Cu_6Sr[(S,S)\text{-Mecysmox}]_3(OH)_2(H_2O)\}$ (Mecysmox = bis[*S*-methylcysteine]oxalyl diamide) (Fig. 10a), features a good number of dimethyl thioether groups decorating their channels, similarly to that observed previously for *L*-methionine MOF. This permits the application of the formerly presented two-step PS[106] strategy, in this case, for the synthesis/stabilization of these Pd^0_1 SACs within their channels (Fig. 10b,c). With that purpose, first, Pd^{2+} cations are introduced within MOF's channels and anchored in specific positions of the channels by interacting with sulfur-containing groups (Fig. 10b) –similarly to that observed with Pt^{II} cations and thioether groups in *L*-methionine MOF (Fig. 8a). Then, the concomitant *in-situ* reduction of Pd^{2+} cations yielded Pd^0_1 SACs homogeneously distributed along the channels of the MOF (Fig. 10c). Remarkably, the high crystallinity[26,27,84,107–109] of this MOF allowed to follow, again, the whole PS process by SCXRD.

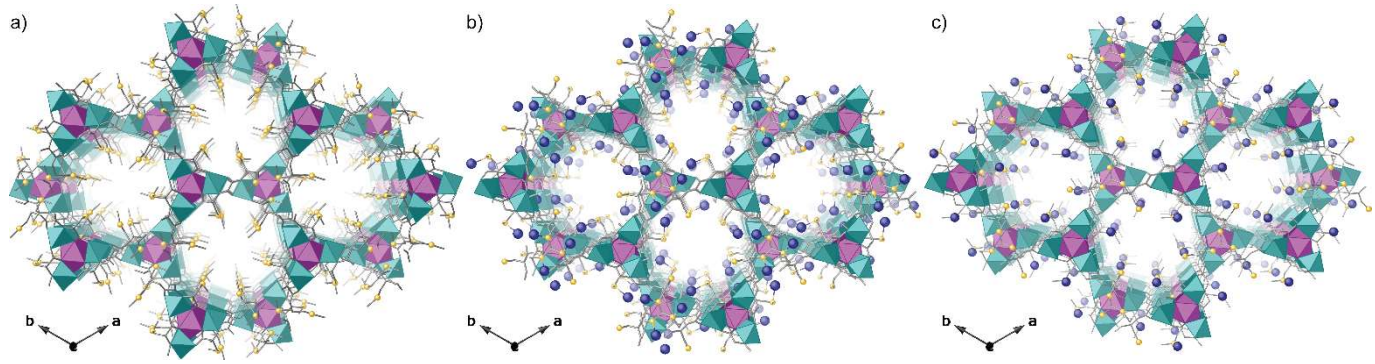

Fig. 10. Crystal structures of $\{Cu_6Sr[(S,S)\text{-Mecysmox}]_3(OH)_2(H_2O)\}$ (a), Pd^{II}_2@MOF (b) and Pd^0_1@MOF (c), determined by single-crystal X-ray diffraction. Copper and strontium atoms from the network are represented by cyan and purple polyhedra, respectively, whereas organic ligands are depicted as grey sticks. Yellow and blue spheres represent S and Pd atoms, respectively. Dashed lines represent the Pd···S interactions.

At this point, a question arises, why Pd SACs are formed in one scenario and Pt_2 SNMCs are formed in the other, considering that metal loading is identical in both cases? The answer comes from the distinct features of each thioether-containing MOF, prepared from *S*-methyl-*L*-cysteine and *L*-methionine, respectively. Indeed, we strongly believe that the distinct length and flexibility of these thioalkyl groups decorating MOFs channels are at the origin of the different nuclearity observed. So, we hypothesize that thioether groups play a dual role in the SAC/SNMCs formation. First, retaining metal cations after insertion process. Then, taking advantage of the different length and high degree of flexibility of thioether residues, getting together or isolating metal species. In this sense, they can be capable to approach two Pt^{II} cations to form dinuclear SNMCs in *L*-methionine MOF (Fig. 11a). Conversely, the shorter length of thioether groups in *S*-methyl-*L*-cysteine (Fig. 11b) prevents Pd^{II} cations to get close enough to form SNMCs, and consequently, SACs are formed instead.

Focusing on catalytic properties of resulting ligand-free Pd^0_1 SACs, they were capable to efficiently catalyse, and with much higher recyclability to their analogues formed in solution, the direct aerobic conversion of benzyl alcohols to benzoic acids without ligands, additives or solvents. Overall, this work showed a straightforward manner to obtain, in large scale, well-defined naked SACs, whose formation mechanism could be also proposed with the help of SCXRD, that can be tentatively used in industrially important catalytic reactions.

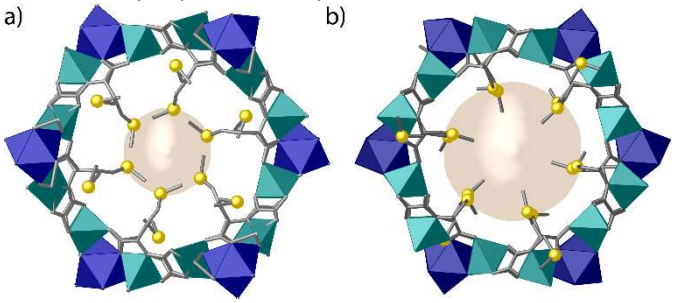

Fig. 11. Crystal structure of one single channel of $\{Cu_6Ca[(S,S)\text{-methox}]_3(OH)_2(H_2O)\}$ (a) and $\{Cu_6Sr[(S,S)\text{-Mecysmox}]_3(OH)_2(H_2O)\}$ (b) emphasizing the different length of thioether groups.

5. MOF-driven self-assembly of SCCs

Alternatively to the controlled synthesis of SACs/SNMCs, the great physicochemical and crystallinity features of selected MOFs as chemical nanoreactors could be exploited for the solid-state self-assembly of unprecedented SCCs –otherwise not accessible– (Fig. 3b), and with outstanding structural stability and catalytic properties –when compared with traditional SCCs assembled in homogeneous solution.[53,74,110–113] This would enable to take advantage of the catalytic potential of pivotal metal atoms constituting the supramolecular assembly, and consequently, further expand the scope of supramolecular catalysis.

In this context, the goodness of the proposed synthetic strategy has been successfully validated for the preparation of several SCCs with distinct nuclearity within the channels of MOF $[Pd^{II}(NH_3)_4][Pd^{II}_2(\mu\text{–}O)(NH_3)_6)(NH_4)_2]_{0.5}\{Ni^{II}_4[Cu^{II}_2(Me_3mpba)_2]_3\}$, obtained after PS cation exchange of Ni^{II} cations by $[Pd^{II}(NH_3)_4]^{2+}$ ones on $Ni^{II}_2\{Ni^{II}_4[Cu^{II}_2(Me_3mpba)_2]_3\}$ MOF (Fig. 7b).[109] In particular, in our first contribution, we were able to report the *in-situ* heterogeneous self-assembly within MOF channels of Pd_8^{II} square metal-organic polygon, when using the linear linker 1,2-di(pyridine-4-yl)ethyne (L_1), meanwhile with the tripodal bent ligand methyl 3,5-bis(pyridine-4-ylethynyl)benzoate (L_2) a discrete water-assisted Pd_{16}^{II} supramolecular cage was obtained (Figs. 11b and 11c).[109]

Remarkably, despite the reasonable difficulties associated with the precise characterisation of the final SCCs@MOF –due to the intrinsic complex nature of such hybrid systems–, the structural robustness and high crystallinity of the MOF selected as chemical nanoreactor results of key importance. This enable, for the first time, the use of SCXRD as basic characterization tool, providing a direct visualization of *in-situ* heterogenous self-assembled SCCs within MOFs channels (Fig. 12). Indeed, this crystallographic study allowed us to obtain unique snapshots of the synergistic interactions established between SCCs and the functionalities decorating the MOF channels, which inherently translate to an improved structural robustness of the assembled supramolecular assemblies mechanically bonded to the MOF network (Fig. 12).

In this connection, the synergistic hybridization of SCCs and MOFs was traduced in remarkable metal-based catalytic properties of pivotal metal atoms constituting the SCCs. Thus, we observed that SCCs@MOF catalyse efficiently the coupling of boronic acids and/or alkynes, with better catalytic conversions and selectivities than standard homogenous Pd catalysts, and, even more relevantly, retaining their structural integrity. This contrasts with the results of traditional homogenous phase assembled SCCs, which tend to decompose under relevant working conditions. Thus, the assembled SCCs@MOF validate the functionality improvement aim of SCCs envisage when we start to develop this supramolecular facet of MOFs as chemical nanoreactors.

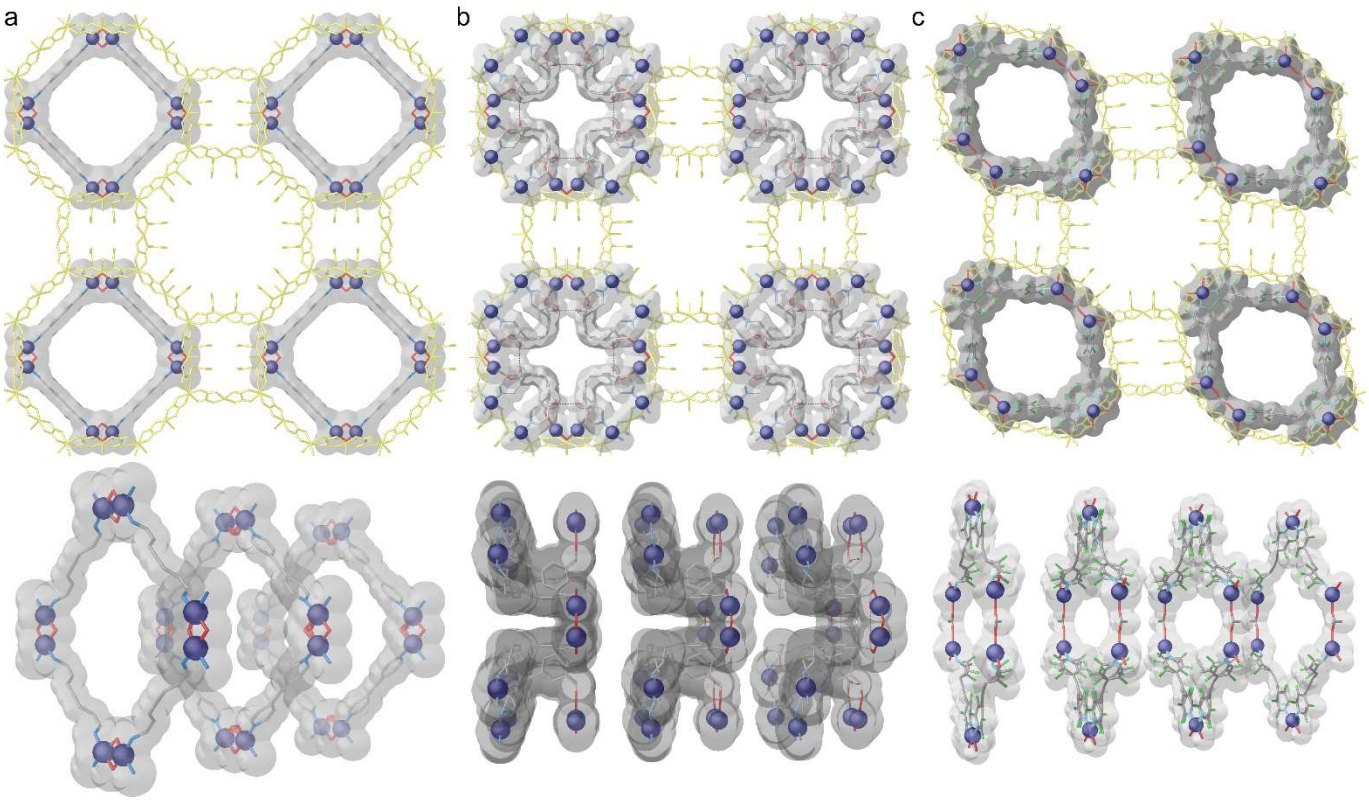

Fig. 12. Crystal structures of host-guest aggregates Pd_8@MOF (a), Pd_{16}@MOF (b) and Pd_6@MOF (c). MOF framework is depicted as yellow sticks and SCCs are showed with surfaces for the sake of clarity. Bottom images show in detail Pd_8 (a), Pd_{16} (b) and Pd_6 (c) SCCs.

Following the same approach, more recently we were able to expand the family of known SCCs@MOFs using linear dipyridyl linkers, related to L_1, but with different number of fluorine substituents. In particular, the fully fluorinated ligand, bis (2,3,5,6-tetrafluorofluoro-pyridin-4-yl)acetylene (L_3), allow us to synthesise and precisely characterise by SCXRD a Pd_6^{II} square metal-organic polygon, which show efficient catalytic behaviour in the aerobic oxidation of aliphatic alcohols to carboxylic acids without any additive.[114] This work nicely illustrated the dual role of MOFs as chemical nanoreactors, enabling the formation of SCCs, that in homogenous phase could not be assembled due to the poor sigma-donor ability of L_3, and transferring stability from the MOF to the assembled SCC, through weak supramolecular interactions, which make possible to fully take advantage of the electrophilic potential of palladium cations constituting the SCC.

Finally, it is worthy to compare the results obtained with related linear linkers L_1 and L_3. Despite it could be assumed, a priori, that ligands with the same donor atoms and at the same distances have to render isoreticular SCC, the experience once again teach us that even small changes in a ligand –distinct functionalization– can reject our assumptions and illustrated us with novel assemblies, which constitute the necessary fuel to keep investigating this recently born supramolecular research field at the interface between SCC and MOFs.

6. Characterization techniques

Taking advantage of the high robustness and crystallinity of selected MOFs as chemical nanoreactors, we could use single-crystal X-ray diffraction (SCXRD) as basic characterization technique, which allowed us to get unique snapshots of the species constructed within MOFs channels, their location and the stabilizing interactions established between them and the functional groups decorating the MOF pores. Nevertheless, the precise characterization of such complex assemblies, as well as the validation of the results obtained by SCXRD, required the implication of a wide range of physical techniques. Thus, thermogravimetric analysis is commonly used to help to establish the solvent content, which is somehow difficult to be ascertained by SCXRD due to intrinsic disorders of such complex structures. Scanning-electron and particularly transmission electron microscopy allowed to observe the homogeneous distribution of metals species and further support the presence

of SNMCs and SACs, respectively. The ratio of the different metal species could be ascertained by inductively coupled plasma-mass spectrometry and scanning electron microscopy with energy dispersive X-ray spectroscopy, allowing to have a double-check of this important feature. Also, necessary is X-ray photoelectron spectroscopy, which is routinary used to help to establish the oxidation state of the formed species. This is of paramount importance thinking toward catalytic applications. N_2 adsorption isotherms and powder X-ray diffraction, in combination, are regularly used to characterise the porosity and robustness of the final assemblies, consequently reflecting the accessible pore space for substrates and the great stability of these materials.

Here, it is worthy to remark, that the materials presented in this feature article represent a beautiful exception among other reported ones, where the characterisation is more frequently associated to a multi-technique approach and not as the one followed by our group, where SCXRD is the main techniques and the others give complementary information. Thus, obtaining a more complete characterisation of the resulting assemblies.

7. Conclusions and outlook

The advantages that metal-organic frameworks (MOFs) can offer when used as chemical nanoreactors to construct unique catalytically-active metal species, such as ligand-free single atom catalysts (SACS), subnanometer metal nanoclusters (SNMCs) and supramolecular coordination complexes (SCCs), have been outlined in this feature article.

The general synthetic strategy has been described, and it can be divided in two main blocks: First, the synthesis/selection of suitable MOFs, which constitutes a crucial step for their successful use as a chemical nanoreactor. Selected MOFs must be highly robust, to resist the formation process of metal species within their pores, and highly crystalline, to allow the application of SCXRD as definitive characterization tool to unveil the nature of formed species. Moreover, MOFs channels must possess appropriate functionalities to anchor/control the number of metal cations, somehow determining the nuclearity of final metal species.

Once MOFs with suitable characteristics are prepared, then, they can be used as chemical nanoreactors to construct desired metal species (SACs/SNMCs and SCCs) by applying solid-state post-synthetic methodologies (PSMs). Another crucial point for the success of this strategy relies on an accurate control of the metal cations that are inserted within the functional constrained space provided by the pores. This is controlled by the charge of the MOF, if it is anionic, and/or the functionalities decorating the channels, which must be capable to retain only a certain amount of metals. Once this limited number of metal cations are inserted and homogeneously distributed within the pores, the second PS step occurs: (*i*) a reduction process in the case of SACs/SNMCs or (*ii*) the insertion of suitable ligands to self-assemble with pre-inserted metals to form SCCs.

In particular, we have proven in recent years that oxamate- and oxamidate ligands, derived from robust aromatic amines or from biomolecules, such as chiral amino acids (Fig. 4), are suitable candidates to synthesise MOFs capable to act as chemical nanoreactors –as they fulfil all requirements, *i.e*. high crystallinity and robustness, as well as the possibility to fine-tune the functionalities decorating their pores, enabling to enhance the affinity for target metal cations. In so doing, we have reported the MOF-driven preparation of highly stable and well-defined ligand-free SACs (Pd^0_1 and Pt^{1+}_1) and homometallic SNMCs (Ag^0_2, Pt^0_2 and $[Pd_4]^{2+}$) and SCCs (Pd_6@MOF, Pd_8@MOF and Pd_{16}@MOF), whose crystal structure could be unveiled by SCXRD, exhibiting outstanding catalytic properties, which are summarised in Table 1. Moreover, given the unique electronic structures of these small metal nanosized species (homo- and heterometallic SACs and SNMCs), they are also expected to be relevant in other important research fields such as optics, medicine and different industrial processes.[19,115,116]

Table 1. SNMCs, SACs and SCCs within MOFs channels presented in this feature article and their catalytic application.

Catalyst@MOF	Catalytic reaction	Ref.
$[Pd_4]_{0.5}$@$Na_3^I\{Ni_4^{II}[Cu_2^{II}(Me_3mpba)_2]_3\}$ (Pd_4^{2+} SNMCs)	Buchner ring expansion and carbene insertion reactions	84
$[Ag_2]$@$Ag_2^INa_2^I\{Ni_4^{II}[Cu_2^{II}(Me_3mpba)_2]_3\}$ (Ag_2^0 SNMCs)	Buchner ring expansion	102
$(Pt_2)_{0.5}$-$(Pt^{II}Cl_2)$@$\{Ca^{II}Cu_6^{II}[(S,S)$-methox$]_3(OH)_2(H_2O)\}$ (Pt_2^0 SNMCs)	CO_2 methanation, cyanide production and selective ethylene hydrogenation	103
Pt_1@$Na_3^I\{Ni_4^{II}[Cu_2^{II}(Me_3mpba)_2]_3\}$ (Pt_1^{1+} SACs)	Water-gas shift	104 108
$(Pd_1)_{0.5}([Pd^{II}(H_2O)(NH_3)_3]Cl_2)_{0.5}$@$\{Sr^{II}Cu_6^{II}[(S,S)$-Mecysmox$]_3(OH)_2CH_3OH)\}$ (Pd_1^0 SACs)	Solvent-free aerobic oxidation of alcohols to benzoic acids	105
$[Pd_2^{II}(\mu$-$OH_2)_2(NH_3)_4)]_{0.5}[Pd_8^{II}(\mu$-$OH_2)_8(NH_3)_8(L_1)_4]_{0.125}\{Ni_4^{II}[Cu_2^{II}(Me_3mpba)_2]_3\}$ (Pd_8^{II} SCCs)	Coupling of boronic acids and/or alkynes	109
$[Pd_{16}^{II}(H_2O)_8(NH_3)_{24}(\mu$-$OH_2)_8(H_2O)_{24}(L_2)_4]_{0.125}\{Ni_4^{II}[Cu_2^{II}(Me_3mpba)_2]_3\}$ (Pd_{16}^{II} SCCs)	Coupling of boronic acids and/or alkynes	109
$[Pd^{II}(NH_3)_4)]_{1.5}$ $[Pd_6^{II}(\mu$-$HOAc)_2(H_2O)_{12}(L_3)_4]_{0.08333}\{Ni_4^{II}[Cu_2^{II}(Me_3mpba)_2]_3\}$ (Pd_6^{II} SCCs)	Additive-free aerobic oxidation of aliphatic alcohols to acids	114

Heterometallic SNMCs and SACs

Overall, following this strategy makes possible that the mentioned novel and stable metal species are obtained in a gram-scale, stabilised–without the need of protective ligands in the case of SACs and SNMCs– and properly characterised at the atomic level, which clearly constitute a clear step forward on the synthesis of these species and their possible use in an industrial scale. However, despite such remarkable results, there is still much work to be done to fully implement this technology in the industry. So, much effort is still required to stablish large-scale synthetic protocols of these catalytically active metal species. Moreover, even if remarkable examples of homometallic SNMCs and SCCs have been obtained, no examples of the heterometallic analogues are reported so far, despite this strategy is highly promising for this purpose. In this context, some preliminary results suggest that these oxamato/oxamidate MOFs could be also successful for the *in-situ* preparation of heterometallic SNMCs and SCCs.

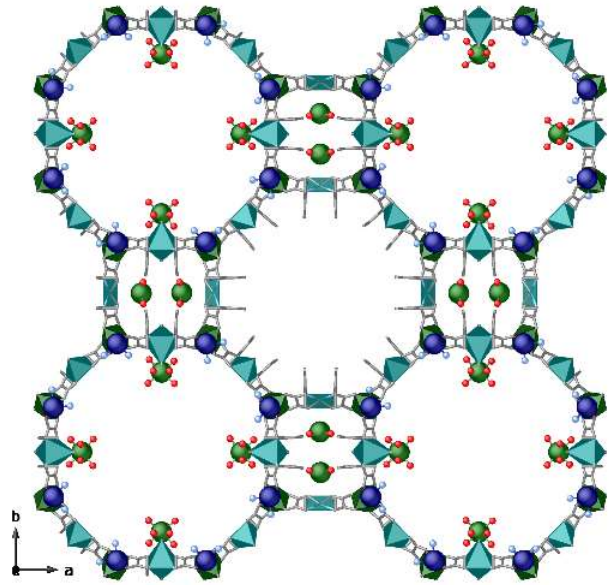

Fig. 13. Crystal structure of $Pd^{II}Ni^{II}$@MOF emphasising the presence of a 50% of Pd^{II} cations (blue spheres) and a 50% of Ni^{II} cations (green spheres) within the channels.

The catalytic activities expected for heterometallic SNMCs may originate a paradigmatic shift within the metal clusters chemistry. Main reasons for such expected thrilling catalytic, but also optical or medical, properties arise from their unique electronic configurations, where a very small number of metals of different nature may exhibit superatom properties, as well as the close proximity between atoms of different nature, which open the possibility to trigger cascade catalytic reactions, in a reminiscent manner to relevant processes in living beings.[117,118] However, so far, the synthesis of these ligand-free heterometallic species, even at a mg scale, has shown even extremely more challenging than homometallic ones. At this respect, we strongly believe that MOF-reactors can be extremely helpful for the preparation of heterometallic SNMCs –and also SCCs. They can be suitable candidates to succeed at this task, considering several features we have already described.

For example, oxamato-based $Ni^{II}_2\{Ni^{II}_4[Cu^{II}_2(Me_3mpba)_2]_3\}$ MOF allows an exquisite control of the number of metal cations that are inserted within its channels, occupying them different specific positions depending on their chemical nature (Figs. 6b,e,h). On this basis, we speculated that we could introduce mixtures of metals of different nature with controlled ratios. This hypothesis has been revealed as successful in a recent publication, where we were capable to replace 50% of Ni^{II} cations hosted in the pores by Pd^{II} ones (Fig. 13). As expected, each distinct metal cation occupies different specific positions, opening the gate for the concomitant introduction of a reducing agent to form heterometallic SNMCs. The same strategy can be, theoretically, designed and applied for the rational preparation of heterometallic SCCs. Taking as the starting point also the introduction of metal cations of different nature within the channels of the MOF, where they occupy different specific positions. Then, after a rigorous analysis of the crystal structure and the positions/distances and encoded coordination preferences of metal cations, suitable ligands could be selected and inserted within the channels to self-assemble forming heterometallic SCCs. In particular, among the plethora of MOFs that could be suitable to synthesise heterometallic SNMCs/SCCs, MTV-MOFs are especially appealing for this purpose as we discuss below.

MTV-MOFs for the preparation of heterometallic SNMCs and SACs

MTV-MOFs, possessing two or more selected functional groups decorating their channels, arise as the more promising materials to synthesis heterometallic SNMCs (Fig. 14a) or SCCs (Fig. 14b). Indeed, if the selected MTV-MOF possess two or more functional groups (Fig. 6), each one having higher affinity for different metal cations, the first step of the PS strategy can be achieved easier. So, the approach consists of introducing, simultaneously or not, a mixture of different metals within the MTV-MOF channels, expecting that a recognition process takes place and each metal occupy a predetermined specific position (Fig. 14 middle). Then, reducing agents or the insertion of appropriate ligands should lead to the direct formation of heterometallic SNMCs (Fig. 14a) or SCCs (Fig. 14b).

The results presented in this feature article are just a small sample of the great undisclosed potential of MOFs as chemical nanoreactors. Thus, it is needed the ingenuous implication of researchers working in the field to further expand this booming area of research, which undoubtedly would trigger novel unexpected results and it will get us closer to fully understand relevant ideas, such the factors influencing the atomicity and topology of prepared SNMCs/SCCs and their relationship with their functionality. We expect that this manuscript acts as the spark to stimulate researchers to grow this research area, still in its infancy.

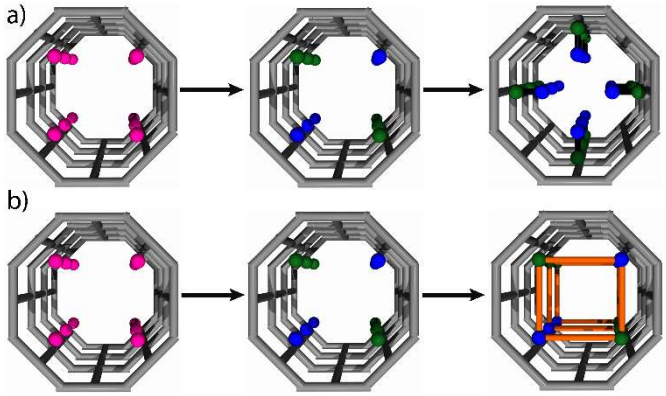

Fig. 14. Postsynthetic strategy for the MOF-driven preparation of heterometallic SNMCs (a) and SCCs (b) using MTV-MOFs.

Author Contributions

EP and J.F.-S. wrote the first draft of the manuscript, and all the authors revised the draft and approved the final version of the manuscript.

Conflicts of interest

There are no conflicts to declare.

Acknowledgements

This work was supported by the MICINN (Spain) (Projects PID2019−104778GB−I00, PID2020-115100GB-I00, and Exc ellence Unit “Maria de Maeztu” CEX2019−000919−M) and the Ministero dell’Istruzione, dell’Università e della Ricerca (Italy). The work has also been funded by Generalitat Valenciana, Prometeo Grupos de Investigación de Excelencia (PROMETEU/2021/054). D.A. acknowledges the financial support of the Fondazione CARIPLO / “Economia Circolare: ricerca per un futuro sostenibile” 2019, Project code: 2019–2090, MOCA. Thanks are also extended to the 2019 Post–doctoral Junior Leader–Retaining Fellowship, la Caixa Foundation (ID100010434 and fellowship code LCF/BQ/PR19/11700011), the “Generalitat Valenciana” (SEJI/2020/034) and the “Ramón y Cajal” program (J.F.–S.). E.P. acknowledges the financial support of the European Research Council under the European Union's Horizon 2020 research and innovation programme / ERC Grant Agreement No 814804, MOF–reactors.

Notes and references

1 D. Bradshaw, J. B. Claridge, E. J. Cussen, T. J. Prior and M. J. Rosseinsky, *Acc. Chem. Res.*, 2005, **38**, 273–282.

2 S. Kitagawa and R. Matsuda, *Coord. Chem. Rev.*, 2007, **251**, 2490–2509.

3 G. Férey, *Chem. Soc. Rev.*, 2008, **37**, 191–214.

4 J. R. Long and O. M. Yaghi, *Chem. Soc. Rev.*, 2009, **38**, 1213–4.

5 H. Furukawa, K. E. Cordova, M. O’Keeffe and O. M. Yaghi, *Science*, 2013, **341**, 974.

6 O. M. Yaghi, M. O’Keeffe, N. W. Ockwig, H. K. Chae, M. Eddaoudi and J. Kim, *Nature*, 2003, **423**, 705–14.

7 S. Kitagawa, R. Kitaura and S. Noro, *Angew. Chemie Int. Ed.*, 2004, **43**, 2334–2375.

8 Z. Chen, P. Li, R. Anderson, X. Wang, X. Zhang, L. Robison, L. R. Redfern, S. Moribe, T. Islamoglu, D. A. Gómez-Gualdrón, T. Yildirim, J. F. Stoddart and O. K. Farha, *Science*, 2020, **368**, 297–303.

9 L. S. Xie, G. Skorupskii and M. Dincă, *Chem. Rev.*, 2020, **120**, 8536–8580.

10 Q. Hu, J. Yu, M. Liu, A. Liu, Z. Dou and Y. Yang, *J. Med. Chem.*, 2014, **57**, 5679–5685.

11 Y. Inokuma, T. Arai and M. Fujita, *Nat. Chem.*, 2010, **2**, 780–783.

12 M. Mon, R. Bruno, J. Ferrando-Soria, D. Armentano and E. Pardo, *J. Mater. Chem. A*, 2018, **6**, 4912–4947.

13 J. Lee, O. K. Farha, J. Roberts, K. a Scheidt, S. T. Nguyen and J. T. Hupp, *Chem. Soc. Rev.*, 2009, **38**, 1450–1459.

14 D. Yang and B. C. Gates, *ACS Catal.*, 2019, **9**, 1779–1798.

15 G. Lu, S. Li, Z. Guo, O. K. Farha, B. G. Hauser, X. Qi, Y. Wang, X. Wang, S. Han, X. Liu, J. S. DuChene, H. Zhang, Q. Zhang, X. Chen, J. Ma, S. C. J. Loo, W. D. Wei, Y. Yang, J. T. Hupp and F. Huo, *Nat. Chem.*, 2012, **4**, 310–316.

16 M. Kalaj and S. M. Cohen, *ACS Cent. Sci.*, 2020, **6**, 1046–1057.

17 W. Xu, K. B. Thapa, Q. Ju, Z. Fang and W. Huang, *Coord. Chem. Rev.*, 2018, **373**, 199–232.

18 S. Wang, C. M. McGuirk, A. D’Aquino, J. A. Mason and C. A. Mirkin, *Adv. Mater.*, 2018, **30**, 1800202.

19 J. Yu, C. Mu, B. Yan, X. Qin, C. Shen, H. Xue and H. Pang, *Mater. Horizons*, 2017, **4**, 557–569.

20 Q. Yang, Q. Xu and H.-L. Jiang, *Chem. Soc. Rev.*, 2017, **46**, 4774–4808.

21 G. Li, S. Zhao, Y. Zhang and Z. Tang, *Adv. Mater.*, 2018, **30**, 1800702.

22 S. Jeoung, S. Kim, M. Kim and H. R. Moon, *Coord. Chem. Rev.*, 2020, **420**, 213377.

23 C. Wang, Z. Xie, K. E. DeKrafft and W. Lin, *J. Am. Chem. Soc.*, 2011, **133**, 13445–13454.

24 C. Wang, J.-L. Wang and W. Lin, *J. Am. Chem. Soc.*, 2012, **134**, 19895–19908.

25 A. Fateeva, P. A. Chater, C. P. Ireland, A. A. Tahir, Y. Z. Khimyak, P. V. Wiper, J. R. Darwent and M. J. Rosseinsky, *Angew. Chem. Int. Ed.*, 2012, **51**, 7440–7444.

26 M. Mon, R. Adam, J. Ferrando−Soria, A. Corma, D. Armentano, E. Pardo and A. Leyva−Pérez, *ACS Catal.*, 2018, **8**, 10401–10406.

27 M. Tejeda-Serrano, M. Mon, B. Ross, F. Gonell, J. Ferrando-Soria, A. Corma, A. Leyva-Pérez, D. Armentano and E. Pardo, *J. Am. Chem. Soc.*, 2018, **140**, 8827–8832.

28 S. Li, X. Tan, M. Yue, L. Zhang, D. Chai, W. Wang, H. Pan, L. Fan and C. Zhao, *Chem. Commun.*, 2020, **56**, 15177–15180.

29 S. Li, L. Zhang, Y. Lan, K. P. O’Halloran, H. Ma and H. Pang, *Chem. Commun.*, 2018, **54**, 1964–1967.

30 T. Kitao, Y. Zhang, S. Kitagawa, B. Wang and T. Uemura,

Chem. Soc. Rev., 2017, **46**, 3108–3133.
31 S. Mochizuki, T. Kitao and T. Uemura, *Chem. Commun.*, 2018, **54**, 11843–11856.
32 M. Kalaj, K. C. Bentz, S. Ayala, J. M. Palomba, K. S. Barcus, Y. Katayama and S. M. Cohen, *Chem. Rev.*, 2020, **120**, 8267–8302.
33 Y. Inokuma, M. Kawano and M. Fujita, *Nat. Chem.*, 2011, **3**, 349–358.
34 Y. Inokuma, S. Yoshioka, J. Ariyoshi, T. Arai, Y. Hitora, K. Takada, S. Matsunaga, K. Rissanen and M. Fujita, *Nature*, 2013, **495**, 461–466.
35 L. M. Hayes, C. E. Knapp, K. Y. Nathoo, N. J. Press, D. A. Tocher and C. J. Carmalt, *Cryst. Growth Des.*, 2016, **16**, 3465–3472.
36 L. M. Hayes, N. J. Press, D. A. Tocher and C. J. Carmalt, *Cryst. Growth Des.*, 2017, **17**, 858–863.
37 K. Rissanen, *Chem. Soc. Rev.*, 2017, **46**, 2638–2648.
38 M. Mon, R. Bruno, J. Ferrando-Soria, L. Bartella, L. Di Donna, M. Talia, R. Lappano, M. Maggiolini, D. Armentano and E. Pardo, *Mater. Horizons*, 2018, **5**, 683–690.
39 M. Mon, J. Ferrando-Soria, M. Verdaguer, C. Train, C. Paillard, B. Dkhil, C. Versace, R. Bruno, D. Armentano and E. Pardo, *J. Am. Chem. Soc.*, 2017, **139**, 8098–8101.
40 P. Li, N. A. Vermeulen, C. D. Malliakas, D. A. Gómez-Gualdrón, A. J. Howarth, B. L. Mehdi, A. Dohnalkova, N. D. Browning, M. O'Keeffe and O. K. Farha, *Science*, 2017, **356**, 624–627.
41 H. Jiang, J. Jia, A. Shkurenko, Z. Chen, K. Adil, Y. Belmabkhout, L. J. Weselinski, A. H. Assen, D.-X. Xue, M. O'Keeffe and M. Eddaoudi, *J. Am. Chem. Soc.*, 2018, **140**, 8858–8867.
42 H.-F. Wang, L. Chen, H. Pang, S. Kaskel and Q. Xu, *Chem. Soc. Rev.*, 2020, **49**, 1414–1448.
43 K. Shen, X. Chen, J. Chen and Y. Li, *ACS Catal.*, 2016, **6**, 5887–5903.
44 L. Zou, Y. Wei, C. Hou, C. Li and Q. Xu, *Small*, 2021, **17**, 2004809.
45 L. Hu, W. Li, L. Wang and B. Wang, *EnergyChem*, 2021, **3**, 100056.
46 J. Juan-Alcañiz, E. V Ramos-Fernandez, F. Kapteijn and J. Gascon, in *RSC Catalysis Series*, 2013, vol. 12, pp. 310–343.
47 Z. Li, S. Ji, Y. Liu, X. Cao, S. Tian, Y. Chen, Z. Niu and Y. Li, *Chem. Rev.*, 2020, **120**, 623–682.
48 X.-F. Yang, A. Wang, B. Qiao, J. Li, J. Liu and T. Zhang, *Acc. Chem. Res.*, 2013, **46**, 1740–1748.
49 N. Wang, Q. Sun and J. Yu, *Adv. Mater.*, 2019, **31**, 1803966.
50 M. Boronat, A. Leyva-Pérez and A. Corma, *Acc. Chem. Res.*, 2014, **47**, 834–844.
51 C. M. Hong, R. G. Bergman, K. N. Raymond and F. D. Toste, *Acc. Chem. Res.*, 2018, **51**, 2447–2455.
52 W. Liu and J. F. Stoddart, *Chem*, 2021, **7**, 919–947.
53 G. Vantomme and E. W. Meijer, *Science*, 2019, **363**, 1396–1397.
54 S. G. Davey, *Nat. Rev. Chem.*, 2020, **4**, 440–440.
55 B. Ni and X. Wang, *Chem. Sci.*, 2016, **7**, 3978–3991.
56 J. PEREZJUSTE, I. PASTORIZASANTOS, L. LIZMARZAN and P. MULVANEY, *Coord. Chem. Rev.*, 2005, **249**, 1870–1901.
57 M. Grzelczak, J. Pérez-Juste, P. Mulvaney and L. M. Liz-Marzán, *Chem. Soc. Rev.*, 2008, **37**, 1783.
58 L. Xu, W. Ma, L. Wang, C. Xu, H. Kuang and N. A. Kotov, *Chem. Soc. Rev.*, 2013, **42**, 3114.
59 Z. Luo, K. Zheng and J. Xie, *Chem. Commun.*, 2014, **50**, 5143–5155.
60 K. Ding, A. Gulec, A. M. Johnson, N. M. Schweitzer, G. D. Stucky, L. D. Marks and P. C. Stair, *Science*, 2015, **350**, 189–192.
61 G. Chen, I. Roy, C. Yang and P. N. Prasad, *Chem. Rev.*, 2016, acs.chemrev.5b00148.
62 T.-H. Shin, Y. Choi, S. Kim and J. Cheon, *Chem. Soc. Rev.*, 2015, **44**, 4501–4516.
63 L. Shang, S. Dong and G. U. Nienhaus, *Nano Today*, 2011, **6**, 401–418.
64 A. Leyva-Pérez, A. Doménech-Carbó and A. Corma, *Nat. Commun.*, 2015, **6**, 6703.
65 N. Wang, Q. Sun, R. Bai, X. Li, G. Guo and J. Yu, *J. Am. Chem. Soc.*, 2016, **138**, 7484–7487.
66 J. Oliver-Meseguer, J. R. Cabrero-Antonino, I. Dominguez, A. Leyva-Perez and A. Corma, *Science*, 2012, **338**, 1452–1455.
67 A. M. Argo, J. F. Odzak, F. S. Lai and B. C. Gates, *Nature*, 2002, **415**, 623–626.
68 K. Okamoto, R. Akiyama, H. Yoshida, T. Yoshida and S. Kobayashi, *J. Am. Chem. Soc.*, 2005, **127**, 2125–2135.
69 N. Vilar-Vidal, J. Rivas and M. A. López-Quintela, *ACS Catal.*, 2012, **2**, 1693–1697.
70 J. Oliver-Meseguer, A. Leyva-Pérez and A. Corma, *ChemCatChem*, 2013, **5**, 3509–3515.
71 A. Corma, P. Concepción, M. Boronat, M. J. Sabater, J. Navas, M. J. Yacaman, E. Larios, A. Posadas, M. A. López-Quintela, D. Buceta, E. Mendoza, G. Guilera and A. Mayoral, *Nat. Chem.*, 2013, **5**, 775–781.
72 J. Oliver-Meseguer, A. Leyva-Pérez, S. I. Al-Resayes and A. Corma, *Chem. Commun.*, 2013, **49**, 7782.
73 A. Leyva-Pérez, J. Oliver-Meseguer, P. Rubio-Marqués and A. Corma, *Angew. Chem. Int. Ed.*, 2013, **52**, 11554–11559.
74 J.-M. Lehn, *Supramolecular Chemistry*, Wiley, 1995.
75 J. Meeuwissen and J. N. H. Reek, *Nat. Chem.*, 2010, **2**, 615–621.
76 H. Wang, Z. Shi, J. Yang, T. Sun, B. Rungtaweevoranit, H. Lyu, Y. Zhang and O. M. Yaghi, *Angew. Chem. Int. Ed.*, 2021, **60**, 3417–3421.
77 T. Grancha, A. Acosta, J. Cano, J. Ferrando-Soria, B. Seoane, J. Gascon, J. Pasán, D. Armentano and E. Pardo, *Inorg. Chem.*, 2015, **54**, 10834–10840.
78 H. Yang, F. Peng, A. N. Hong, Y. Wang, X. Bu and P. Feng, *J. Am. Chem. Soc.*, 2021, **143**, 14470–14474.
79 D. Feng, W.-C. Chung, Z. Wei, Z.-Y. Gu, H.-L. Jiang, Y.-P. Chen, D. J. Darensbourg and H.-C. Zhou, *J. Am. Chem. Soc.*, 2013, **135**, 17105–17110.
80 S. B. Kalidindi, S. Nayak, M. E. Briggs, S. Jansat, A. P. Katsoulidis, G. J. Miller, J. E. Warren, D. Antypov, F. Corà, B. Slater, M. R. Prestly, C. Martí-Gastaldo and M. J. Rosseinsky, *Angew. Chem. Int. Ed.*, 2015, **54**, 221–226.
81 X. Sun, S. Yao, C. Yu, G. Li, C. Liu, Q. Huo and Y. Liu, *J.*

Mater. Chem. A, 2018, **6**, 6363–6369.

82 N. M. Padial, J. Castells-Gil, N. Almora-Barrios, M. Romero-Angel, I. da Silva, M. Barawi, A. García-Sánchez, V. A. de la Peña O'Shea and C. Martí-Gastaldo, *J. Am. Chem. Soc.*, 2019, **141**, 13124–13133.

83 S. Wang, M. Cabrero-Antonino, S. Navalón, C. Cao, A. Tissot, I. Dovgaliuk, J. Marrot, C. Martineau-Corcos, L. Yu, H. Wang, W. Shepard, H. García and C. Serre, *Chem*, 2020, **6**, 3409–3427.

84 F. R. Fortea-Pérez, M. Mon, J. Ferrando-Soria, M. Boronat, A. Leyva-Pérez, A. Corma, J. M. Herrera, D. Osadchii, J. Gascon, D. Armentano and E. Pardo, *Nat. Mater.*, 2017, **16**, 760–766.

85 T. Grancha, M. Mon, J. Ferrando-Soria, J. Gascon, B. Seoane, E. V. Ramos-Fernandez, D. Armentano and E. Pardo, *J. Mater. Chem. A*, 2017, **5**, 11032–11039.

86 T. Grancha, J. Ferrando-Soria, J. Cano, P. Amorós, B. Seoane, J. Gascon, M. Bazaga-García, E. R. Losilla, A. Cabeza, D. Armentano and E. Pardo, *Chem. Mater.*, 2016, **28**, 4608–4615.

87 M. Mon, J. Ferrando-Soria, T. Grancha, F. R. Fortea-Pérez, J. Gascon, A. Leyva-Pérez, D. Armentano and E. Pardo, *J. Am. Chem. Soc.*, 2016, **138**, 7864–7867.

88 T. Grancha, M. Mon, J. Ferrando-Soria, D. Armentano and E. Pardo, *Cryst. Growth Des.*, 2016, **16**, 5571–5578.

89 M. Mon, F. Lloret, J. Ferrando-Soria, C. Martí-Gastaldo, D. Armentano and E. Pardo, *Angew. Chem. Int. Ed.*, 2016, **55**, 11167–11172.

90 M. Viciano-Chumillas, X. Liu, A. Leyva-Pérez, D. Armentano, J. Ferrando-Soria and E. Pardo, *Coord. Chem. Rev.*, 2022, **451**, 214273.

91 J. Jiao, W. Gong, X. Wu, S. Yang and Y. Cui, *Coord. Chem. Rev.*, 2019, **385**, 174–190.

92 A. Helal, Z. H. Yamani, K. E. Cordova and O. M. Yaghi, *Natl. Sci. Rev.*, 2017, **4**, 296–298.

93 T. M. Osborn Popp and O. M. Yaghi, *Acc. Chem. Res.*, 2017, **50**, 532–534.

94 M. Mon, R. Bruno, E. Tiburcio, P.-E. Casteran, J. Ferrando-Soria, D. Armentano and E. Pardo, *Chem. Eur. J.*, 2018, **24**, 17712–17718.

95 M. Baratta, T. F. Mastropietro, R. Bruno, A. Tursi, C. Negro, J. Ferrando-Soria, A. I. Mashin, A. Nezhdanov, F. P. Nicoletta, G. De Filpo, E. Pardo and D. Armentano, *ACS Appl. Nano Mater.*, 2022, **5**, 5223–5233.

96 R. Bruno, M. Mon, P. Escamilla, J. Ferrando-Soria, E. Esposito, A. Fuoco, M. Monteleone, J. C. Jansen, R. Elliani, A. Tagarelli, D. Armentano and E. Pardo, *Adv. Funct. Mater.*, 2021, **31**, 2008499.

97 A. Tursi, T. F. Mastropietro, R. Bruno, M. Baratta, J. Ferrando-Soria, A. I. Mashin, F. P. Nicoletta, E. Pardo, G. De Filpo and D. Armentano, *Adv. Mater. Interfaces*, 2021, **8**, 2100730.

98 M. Mon, X. Qu, J. Ferrando-Soria, I. Pellicer-Carreño, A. Sepúlveda-Escribano, E. V. Ramos-Fernandez, J. C. Jansen, D. Armentano and E. Pardo, *J. Mater. Chem. A*, 2017, **5**, 20120–20125.

99 C. Negro, P. Escamilla, R. Bruno, J. Ferrando-Soria, D. Armentano and E. Pardo, *Chem. Eur. J.*, , DOI:10.1002/chem.202200034.

100 C. Negro, H. Martínez Pérez-Cejuela, E. F. Simó-Alfonso, J. M. Herrero-Martínez, R. Bruno, D. Armentano, J. Ferrando-Soria and E. Pardo, *ACS Appl. Mater. Interfaces*, 2021, **13**, 28424–28432.

101 M. P. Doyle, R. Duffy, M. Ratnikov and L. Zhou, *Chem. Rev.*, 2010, **110**, 704–724.

102 E. Tiburcio, Y. Zheng, M. Mon, N. Martín, J. Ferrando−Soria, D. Armentano, A. Leyva−Pérez and E. Pardo, *Inorg. Chem.*, 2022, **61**, 11796–11802.

103 M. Mon, M. A. Rivero-Crespo, J. Ferrando-Soria, A. Vidal-Moya, M. Boronat, A. Leyva-Pérez, A. Corma, J. C. Hernández-Garrido, M. López-Haro, J. J. Calvino, G. Ragazzon, A. Credi, D. Armentano and E. Pardo, *Angew. Chem. Int. Ed.*, 2018, **57**, 6186–6191.

104 C. Bilanin, E. Tiburcio, J. Ferrando-Soria, D. Armentano, A. Leyva-Pérez and E. Pardo, *ChemCatChem*, 2021, **13**, 1195–1200.

105 E. Tiburcio, R. Greco, M. Mon, J. Ballesteros-Soberanas, J. Ferrando-Soria, M. López-Haro, J. C. Hernández-Garrido, J. Oliver-Meseguer, C. Marini, M. Boronat, D. Armentano, A. Leyva-Pérez and E. Pardo, *J. Am. Chem. Soc.*, 2021, **143**, 2581–2592.

106 M. Viciano-Chumillas, M. Mon, J. Ferrando-Soria, A. Corma, A. Leyva-Pérez, D. Armentano and E. Pardo, *Acc. Chem. Res.*, 2020, **53**, 520–531.

107 T. Grancha, J. Ferrando-Soria, H.-C. Zhou, J. Gascon, B. Seoane, J. Pasán, O. Fabelo, M. Julve and E. Pardo, *Angew. Chem. Int. Ed.*, 2015, **54**, 6521–6525.

108 M. A. Rivero-Crespo, M. Mon, J. Ferrando-Soria, C. W. Lopes, M. Boronat, A. Leyva-Pérez, A. Corma, J. C. Hernández-Garrido, M. López-Haro, J. J. Calvino, E. V. Ramos-Fernandez, D. Armentano and E. Pardo, *Angew. Chem. Int. Ed.*, 2018, **57**, 17094–17099.

109 R. Adam, M. Mon, R. Greco, L. H. G. Kalinke, A. Vidal-Moya, A. Fernandez, R. E. P. Winpenny, A. Doménech-Carbó, A. Leyva-Pérez, D. Armentano, E. Pardo and J. Ferrando-Soria, *J. Am. Chem. Soc.*, 2019, **141**, 10350–10360.

110 A. B. Grommet and J. R. Nitschke, *J. Am. Chem. Soc.*, 2017, **139**, 2176–2179.

111 J. Mosquera, T. K. Ronson and J. R. Nitschke, *J. Am. Chem. Soc.*, 2016, **138**, 1812–1815.

112 S. M. Jansze, G. Cecot, M. D. Wise, K. O. Zhurov, T. K. Ronson, A. M. Castilla, A. Finelli, P. Pattison, E. Solari, R. Scopelliti, G. E. Zelinskii, A. V. Vologzhanina, Y. Z. Voloshin, J. R. Nitschke and K. Severin, *J. Am. Chem. Soc.*, 2016, **138**, 2046–2054.

113 T. K. Ronson, D. A. Roberts, S. P. Black and J. R. Nitschke, *J. Am. Chem. Soc.*, 2015, **137**, 14502–14512.

114 R. Greco, E. Tiburcio-Fortes, A. Fernandez, C. Marini, A. Vidal-Moya, J. Oliver-Meseguer, D. Armentano, E. Pardo, J. Ferrando-Soria and A. Leyva-Pérez, *Chem. Eur. J.*, , DOI:10.1002/chem.202103781.

115 S. Mitchell, R. Qin, N. Zheng and J. Pérez-Ramírez, *Nat. Nanotechnol.*, 2021, **16**, 129–139.

116 P. Falcaro, R. Ricco, A. Yazdi, I. Imaz, S. Furukawa, D.

Maspoch, R. Ameloot, J. D. Evans and C. J. Doonan, *Coord. Chem. Rev.*, 2016, **307**, 237–254.

117 Y. Okamoto and T. R. Ward, in *Comprehensive Supramolecular Chemistry II*, Elsevier, 2017, pp. 459–510.

118 M. Mon, R. Bruno, S. Sanz-Navarro, C. Negro, J. Ferrando-Soria, L. Bartella, L. Di Donna, M. Prejanò, T. Marino, A. Leyva-Pérez, D. Armentano and E. Pardo, *Nat. Commun.*, 2020, **11**, 3080.